

---

**This is an electronic reprint of the original article.**  
**This reprint *may differ from the original in pagination and typographic detail.***

**Author(s):** Capponi, L.; Smith, J. F.; Ruotsalainen, Panu; Scholey, Catherine; Rahkila, Panu; Auranen, Kalle; Bianco, L.; Boston, A. J.; Boston, H. C.; Cullen, D. M.; Derkx, X.; Drummond, M. C.; Grahn, Tuomas; Greenlees, Paul; Grocott, L.; Hadinia, B.; Jakobsson, Ulrika; Joss, D. T.; Julin, Rauno; Juutinen, Sakari; Labiche, M.; Leach, K. G.; Leino, Matti; McPeake, C.; Mulholland, K. F.; Nieminen, Päivi; O'Donnell, D.; Paul, E. S.; Uusitalo, J.

**Title:** Direct observation of the  $Ba\ 114 \rightarrow Xe\ 110 \rightarrow Te\ 106 \rightarrow Sn\ 102$  triple  $\alpha$ -decay chain using position and time correlations

**Year:** 2016

**Version:**

**Please cite the original version:**

Capponi, L., Smith, J. F., Ruotsalainen, P., Scholey, C., Rahkila, P., Auranen, K., Bianco, L., Boston, A. J., Boston, H. C., Cullen, D. M., Derkx, X., Drummond, M. C., Grahn, T., Greenlees, P., Grocott, L., Hadinia, B., Jakobsson, U., Joss, D. T., Julin, R., . . . Uusitalo, J. (2016). Direct observation of the  $Ba\ 114 \rightarrow Xe\ 110 \rightarrow Te\ 106 \rightarrow Sn\ 102$  triple  $\alpha$ -decay chain using position and time correlations. *Physical Review C*, 94(2), Article 024314. <https://doi.org/10.1103/PhysRevC.94.024314>

All material supplied via JYX is protected by copyright and other intellectual property rights, and duplication or sale of all or part of any of the repository collections is not permitted, except that material may be duplicated by you for your research use or educational purposes in electronic or print form. You must obtain permission for any other use. Electronic or print copies may not be offered, whether for sale or otherwise to anyone who is not an authorised user.

# Direct observation of the $^{114}\text{Ba} \rightarrow ^{110}\text{Xe} \rightarrow ^{106}\text{Te} \rightarrow ^{102}\text{Sn}$ triple $\alpha$ -decay chain using position and time correlations

L. Capponi,<sup>1,2,\*</sup> J. F. Smith,<sup>1,2,†</sup> P. Ruotsalainen,<sup>3,‡</sup> C. Scholey,<sup>3</sup> P. Rahkila,<sup>3</sup> K. Auranen,<sup>3,§</sup> L. Bianco,<sup>4</sup> A. J. Boston,<sup>5</sup> H. C. Boston,<sup>5</sup> D. M. Cullen,<sup>6</sup> X. Derkx,<sup>1,2,||</sup> M. C. Drummond,<sup>5</sup> T. Grahn,<sup>3</sup> P. T. Greenlees,<sup>3</sup> L. Grocott,<sup>1,2</sup> B. Hadinia,<sup>7</sup> U. Jakobsson,<sup>3,¶</sup> D. T. Joss,<sup>5</sup> R. Julin,<sup>3</sup> S. Juutinen,<sup>3</sup> M. Labiche,<sup>8</sup> M. Leino,<sup>3</sup> K. G. Leach,<sup>7,\*\*</sup> C. McPeake,<sup>5</sup> K. F. Mulholland,<sup>1,2</sup> P. Nieminen,<sup>3</sup> D. O'Donnell,<sup>1,2</sup> E. S. Paul,<sup>5</sup> P. Peura,<sup>3,††</sup> M. Sandzelius,<sup>3</sup> J. Sarén,<sup>3</sup> B. Saygi,<sup>5</sup> J. Sorri,<sup>3</sup> S. Stolze,<sup>3</sup> A. Thornthwaite,<sup>5</sup> M. J. Taylor,<sup>6</sup> and J. Uusitalo<sup>3</sup>

<sup>1</sup>School of Engineering and Computing, University of the West of Scotland, Paisley PA1 2BE, United Kingdom

<sup>2</sup>Scottish Universities Physics Alliance

<sup>3</sup>Department of Physics, University of Jyväskylä, P.O. Box 35, Jyväskylä FIN-40014, Finland

<sup>4</sup>Department of Physics, University of Guelph, Guelph, Ontario N1G 2W1, Canada

<sup>5</sup>Oliver Lodge Laboratory, University of Liverpool, Liverpool L69 7ZE, United Kingdom

<sup>6</sup>School of Physics and Astronomy, Schuster Building, University of Manchester, Manchester M13 9PL, United Kingdom

<sup>7</sup>Department of Physics, University of Guelph, Guelph, Ontario N1G 2W1, Canada

<sup>8</sup>Nuclear Physics Group, STFC Daresbury Laboratory, Daresbury, Warrington WA4 4AD, United Kingdom

(Received 12 June 2016; published 10 August 2016)

The triple  $\alpha$ -decay chain  $^{114}\text{Ba} \rightarrow ^{110}\text{Xe} \rightarrow ^{106}\text{Te} \rightarrow ^{102}\text{Sn}$  has been directly observed for the first time, following the  $^{58}\text{Ni}(^{58}\text{Ni}, 2n)$  reaction. Implantation of  $^{114}\text{Ba}$  nuclei into a double-sided silicon-strip detector has allowed their  $\alpha$  decays to be correlated in position and time with the  $\alpha$  decays of the daughter ( $^{110}\text{Xe}$ ) and granddaughter ( $^{106}\text{Te}$ ) nuclei. In total, 17 events have been assigned to the  $^{114}\text{Ba} \rightarrow ^{110}\text{Xe} \rightarrow ^{106}\text{Te} \rightarrow ^{102}\text{Sn}$  triple  $\alpha$ -decay chain. The energy of the  $^{114}\text{Ba}$   $\alpha$  decay has been measured to be  $E_\alpha = 3480(20)$  keV, which is 70 keV higher than the previously measured value, and the half-life of  $^{114}\text{Ba}$  has been measured with improved accuracy, to be  $380_{-110}^{+190}$  ms. A revised  $Q_{12\text{C}}$  value of 19 035(45) keV for  $^{114}\text{Ba}$  is presented.

DOI: 10.1103/PhysRevC.94.024314

## I. INTRODUCTION

The study of the different decay modes of the proton-rich nuclei immediately northeast of  $^{100}\text{Sn}$  can be a valuable source of information about nuclear structure and nuclear properties at the boundary of nuclear existence. The island of  $\alpha$ -particle and proton emitters in the light  $52 \leq Z \leq 56$  nuclei [1] is particularly significant in this regard. Excited states of some of these nuclei have been studied by using characteristic  $\alpha$  and proton decays as a tool to select and identify the nuclei of interest using the method of recoil-decay tagging [2–5].  $\alpha$  decays themselves are also a valuable source of information. For example, the energy of an  $\alpha$  particle ( $E_\alpha$ ) can give the difference in mass of the mother and daughter nuclei. Energies,

half-lives ( $T_{1/2}$ ), and  $\alpha$ -decay branching ratios ( $b_\alpha$ ) can be used to extract reduced widths; in the  $N \simeq Z \simeq 50$  region, reduced widths are particularly interesting since the neutrons and protons near the Fermi level can occupy identical  $d_{3/2}$ ,  $d_{5/2}$ , and  $g_{7/2}$  orbitals leading to the possibility of superallowed  $\alpha$  decay [6]. Another interesting aspect in this region is the prediction of cluster radioactivity [7]. It has been widely reported that the most promising candidate for this type of decay in the region is the  $^{12}\text{C}$  decay  $^{114}\text{Ba} \rightarrow ^{102}\text{Sn}$  [8–10], and that the theoretical predictions of the partial half-life depend very sensitively on the  $Q$  value for  $^{12}\text{C}$  emission ( $Q_{12\text{C}}$ ) [8]. The value of  $Q_{12\text{C}}$  is therefore an important quantity in the design of experiments to search for this novel decay mode.

Recent experimental developments, such as triggerless data acquisition [11] and digital signal processing, have enabled significant progress in the study of  $\alpha$  decay in the  $N \simeq Z \simeq 50$  region. For example, the  $^{109}\text{Xe} \rightarrow ^{105}\text{Te} \rightarrow ^{101}\text{Sn}$  decay chain has recently been studied despite the very short half-life of 620(70) ns for  $^{105}\text{Te}$  [12]. Further study of this decay chain in Ref. [13] has revealed interesting information on the ordering of single-particle states in  $^{101}\text{Sn}$ . The known  $\alpha$ -emitting nuclei in the  $A = 100$ –110 region are shown in Fig. 1. In total, there are about 20 nuclei in this region which decay by  $\alpha$ -particle emission. In many cases, the daughters of the  $\alpha$  emitters are also themselves  $\alpha$  emitters, leading to a number of two- $\alpha$ -decay chains. Experimentally, time and position correlations between two  $\alpha$  decays can act as a very sensitive selection tool, particularly when one of the  $\alpha$  decays has a short half-life. Indeed, because this region of  $\alpha$  emitters spans five  $Z$  values ( $52 \leq Z \leq 56$ ) it is possible to have three- $\alpha$ -decay

\*Present address: ELI-NP, Horia Hulubei National Institute of Physics and Nuclear Engineering, 077125 Magurele, Romania.

†John.F.Smith@uws.ac.uk

‡Present address: TRIUMF, 4004 Wesbrook Mall, Vancouver, British Columbia, V6T 2A3, Canada.

§Present address: Physics Division, Argonne National Laboratory, Argonne, Illinois 60439, USA.

||Present address: Johannes Gutenberg-Universität Mainz, 55099 Mainz, Germany.

¶Present address: Helsinki Institute of Physics, University of Helsinki, P.O. Box 64, FIN-00014 Helsinki, Finland.

\*\*Present address: TRIUMF, 4004 Wesbrook Mall, Vancouver, British Columbia, V6T 2A3, Canada.

††Present address: Helsinki Institute of Physics, University of Helsinki, P.O. Box 64, FIN-00014 Helsinki, Finland.

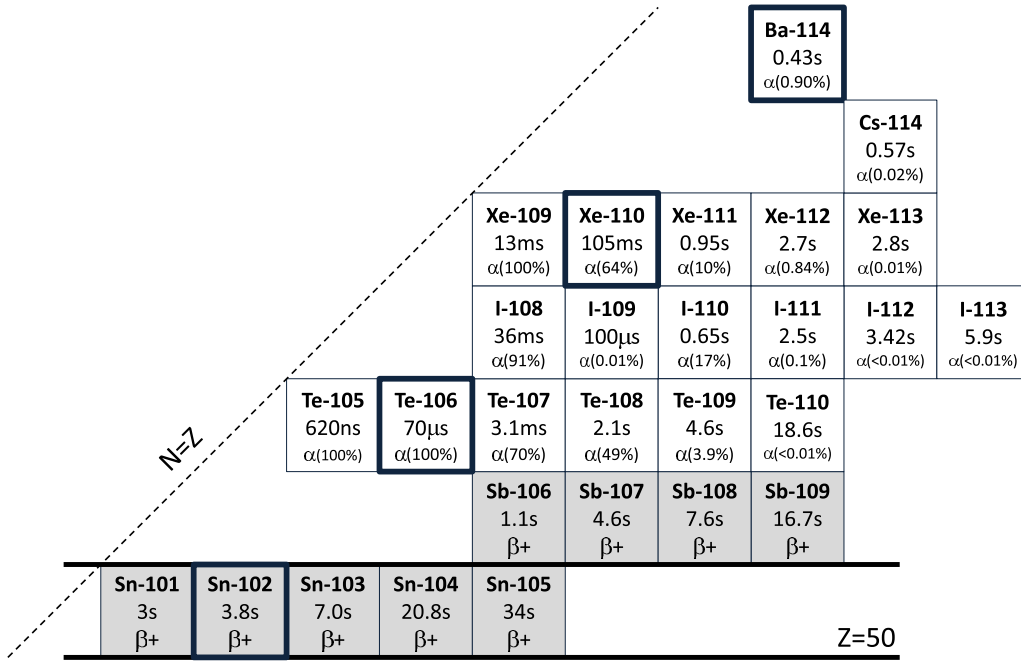


FIG. 1. A chart showing the  $\alpha$ -emitting  $^{52}\text{Te}$ ,  $^{53}\text{I}$ ,  $^{54}\text{Xe}$ ,  $^{55}\text{Cs}$ , and  $^{56}\text{Ba}$  nuclei in the region above the  $N \simeq Z \simeq 50$  shell closures. For each nucleus, the half-life and the  $\alpha$ -decay branching ratio are given. The shaded  $^{50}\text{Sn}$  and  $^{51}\text{Sb}$  nuclei represent the end points of the  $\alpha$ -decay chains; these nuclei decay by  $\beta^+$  emission. Nuclei in the  $^{114}\text{Ba} \rightarrow ^{110}\text{Xe} \rightarrow ^{106}\text{Te} \rightarrow ^{102}\text{Sn}$  decay chain, of interest in this work, are marked with thick black borders. The proximity to  $Z = 50$  and to the  $N = Z$  line is shown.

chains starting from isotopes of barium ( $Z = 56$ ). Presently, the only barium isotope which has been shown to decay by  $\alpha$ -particle emission is  $^{114}\text{Ba}$  [14].

## II. PREVIOUS STUDIES

The nucleus  $^{114}\text{Ba}$  has been the subject of a number of experimental studies in the past 20 years, all of which have used the  $^{58}\text{Ni}(^{58}\text{Ni}, 2n)$  reaction. With stable beams, this reaction offers the only viable possibility of producing  $^{114}\text{Ba}$  with a cross section sufficient for study. In 1993, Oganessian *et al.* [15] reported on an experiment performed using the Dubna U400 cyclotron to search for  $^{12}\text{C}$  emission from  $^{114}\text{Ba}$ . The  $^{58}\text{Ni}$  beam had energy of 280 MeV and polycarbonate track detectors were used to identify the emitted  $^{12}\text{C}$  particles. Several candidate tracks were identified, but the results were inconclusive. However, an upper limit on the  $^{12}\text{C}$  branching ratio ( $b_{^{12}\text{C}}$ ) of  $10^{-4}$  was put forward. Subsequently, two experiments were performed using the online mass separator at the GSI UNILAC by Guglielmetti *et al.* [9,10,16,17]. In that work, a  $^{58}\text{Ni}$  beam with 4.9 MeV/A (284 MeV) was used, for which the cross section was reported to be  $0.2^{+0.13}_{-0.09} \mu\text{b}$ . The experiments used the ISOL technique with the reaction products stopped in a hot catcher, evaporated, ionized, accelerated, and magnetically mass separated. Separation of Ba and Cs ions was achieved using a fluorination technique, in which Cs is suppressed as it does not form fluoride ions. The  $\text{BaF}^+$  ions were caught on a stopper foil at the center of an array of  $\Delta E - E$  silicon-plus-plastic-scintillator telescopes. In the initial experiment [9,10], the observation of three  $^{12}\text{C}$  decay events was reported, but following the second experiment

[16,17] with improved background subtraction, these claims were retracted. In that work, the half-life of  $^{114}\text{Ba}$  was reported to be  $0.43^{+0.30}_{-0.15}$  s and an upper limit of  $b_{^{12}\text{C}} \leq 3.4 \times 10^{-5}$  was given. The  $\alpha$  decay of  $^{114}\text{Ba}$  was reported by Mazzocchi *et al.* in Refs. [14,18]: a dedicated experiment was performed at the GSI UNILAC using the fluorination technique, and the  $\alpha$ -particle energy was reported to be 3410(40) keV, with an  $\alpha$ -decay branch of 0.9(3)%. Also, in that work, the half-life of the daughter nucleus  $^{110}\text{Xe}$  was measured to be  $160^{+290}_{-60}$  ms. It should perhaps be noted here that although the  $\alpha$  decays of  $^{114}\text{Ba}$ ,  $^{110}\text{Xe}$ , and  $^{106}\text{Te}$  were observed, the reaction products were collected on a passive catcher foil, and no position correlations were recorded. Time correlations used to measure the lifetime of  $^{110}\text{Xe}$  were reliant on the purity of the  $\text{BaF}^+$  beam.

In the present work, the  $^{114}\text{Ba}$  nucleus has been produced and the three- $\alpha$ -decay chain, starting with  $^{114}\text{Ba}$  and ending at  $^{102}\text{Sn}$ , has been studied using both position and time correlations between the  $\alpha$  decays of  $^{114}\text{Ba}$ ,  $^{110}\text{Xe}$ , and  $^{106}\text{Te}$ .

## III. EXPERIMENTAL DETAILS

This work reports on results from an experiment carried out using the K130 cyclotron at the Accelerator Laboratory of the University of Jyväskylä Department of Physics. The primary aim of the experiment was to study the excited states and  $\alpha$  decay of  $^{111}\text{Xe}$ , and the experimental conditions were optimized for that purpose; details of the experiment and the results concerning  $^{111}\text{Xe}$  are reported elsewhere [19,20]. A beam of  $^{58}\text{Ni}$  ions, with energy 210 MeV, was incident upon a  $500-\mu\text{g}/\text{cm}^2$   $^{58}\text{Ni}$  target. Prompt  $\gamma$  rays, emitted at the reaction

site, were detected by the Jurogam-II  $\gamma$ -ray spectrometer [21]. Recoiling reaction products were separated from the primary beam by the RITU gas-filled recoil separator [22]. On exit from RITU, the reaction products passed through a multiwire proportional counter (MWPC) before being implanted into one of two adjacent double-sided silicon strip detectors (DSSDs), each of thickness 300  $\mu\text{m}$  and with 40 horizontal (front) strips and 60 vertical (back) strips, giving a total of 4800 DSSD pixels. A planar HPGe detector and three Clover HPGe detectors were placed around the DSSDs. The MWPC, DSSDs, planar HPGe and (focal plane) Clover HPGe detectors are part of the GREAT spectrometer [23]. The Total Data Readout data-acquisition system was used [11], in which a 100-MHz clock provided a time stamp on each detector signal, accurate to the nearest 10 ns. Data were recorded for all detector signals received within a fixed time window around either (a) a signal in the DSSDs (implant or decay) or (b)  $\geq 2$  prompt signals in the Jurogam-II spectrometer. The beam intensity was limited to an average value of 2 pA for the duration of the experiment in order to keep the implantation rate in the DSSD appropriate for implant-decay correlations of  $^{111}\text{Xe}$  ( $T_{1/2} \approx 800$  ms). In total, approximately 1 TB of data were written to disk. The data were analyzed using the GRAIN data analysis package [24]. For the  $^{114}\text{Ba}$  decay results presented here, data from  $\gamma$ -ray detectors were not used; the data are from analysis of the DSSD and MWPC signals.

The DSSDs were initially gain matched using a mixed source of  $^{239}\text{Pu}$ ,  $^{241}\text{Am}$ , and  $^{244}\text{Cm}$ , which emit  $\alpha$  particles with energies in the range of 5 to 6 MeV. In addition to use of the source data, an internal calibration of the DSSDs was performed using the  $^{58}\text{Ni}$  beam, with energy 235 MeV, incident on a natural molybdenum target; the known energies of protons and  $\alpha$  particles emitted by the proton-rich  $^{66}\text{Dy}$ ,  $^{68}\text{Er}$ , and  $^{70}\text{Yb}$  nuclei implanted into the DSSD were then used to calibrate the individual DSSD strips.

#### IV. DATA ANALYSIS AND RESULTS

Implantation events in the DSSDs were identified by demanding a time correlation with a signal from the MWPC (with no energy constraint) or an energy  $\geq 7$  MeV. Conversely, decay events were those with no time-correlated MWPC signal and with energy  $< 7$  MeV. This resulted in  $9 \times 10^8$  implantation events (henceforth referred to as *implants*) and  $2 \times 10^7$  decay events (*decays*) in the DSSDs. In order to identify the implanted nuclear species, a decay with the correct energy was required in the same DSSD pixel as the implant, within a search time period of three or four half-lives. Within three half-lives, 88% of the implants decay; within four half-lives, 94% decay. Consideration was also given to false correlations: a longer half-life gives a higher likelihood of false correlations, in which successive implants occur before the initial implants have decayed. In this work, the average time between implants in each pixel was found to be  $\sim 1.1$  s, but the implantation rate is dependent on position in the DSSD with the highest rates in the central strips and lower rates at the edges. Any search time close to 1 s, or longer, will therefore be susceptible to false correlations, and the number of false correlations will be dependent on position in the DSSD.

The half-lives of nuclei in the  $^{114}\text{Ba} \rightarrow ^{110}\text{Xe} \rightarrow ^{106}\text{Te} \rightarrow ^{102}\text{Sn}$   $\alpha$ -decay chain have previously been measured to be  $T_{1/2}(^{114}\text{Ba}) = 430^{+300}_{-150}$  ms [14],  $T_{1/2}(^{110}\text{Xe}) = 105^{+35}_{-25}$  ms [25], and  $T_{1/2}(^{106}\text{Te}) = 70^{+20}_{-10}$   $\mu\text{s}$  [25]. The relatively long half-lives of  $^{114}\text{Ba}$  and of its daughter  $^{110}\text{Xe}$  mean that any attempts to identify  $^{114}\text{Ba}$  using single  $^{114}\text{Ba}$  or  $^{110}\text{Xe}$   $\alpha$  decays are difficult due to the large number of false correlations.

As stated earlier, the  $\alpha$  emitters in the  $A = 110$  region span the range  $52 \leq Z \leq 56$  (Fig. 1), so any chain of three  $\alpha$  decays in this region must start from an isotope of barium ( $Z = 56$ ). The nucleus  $^{113}\text{Ba}$  has so far not been observed experimentally. The nucleus  $^{115}\text{Ba}$  was identified by Janas *et al.* [17] but in that work no  $\alpha$ -decay branch was identified. In the present reaction, it is very unlikely that  $^{115}\text{Ba}$  will be produced, as this would require  $1n$  evaporation which is expected to be at or below the interaction barrier. The nucleus  $^{113}\text{Ba}$  has been the subject of a dedicated search using the  $^{58}\text{Ni}(^{58}\text{Ni}, 3n)$  reaction, as described in Ref. [14], but no evidence for this nucleus was reported. It can therefore be initially assumed that any observed chain of three  $\alpha$  decays following the  $^{58}\text{Ni}(^{58}\text{Ni})$  reaction is likely to originate from  $^{114}\text{Ba}$ . A three- $\alpha$  requirement can thus be used as an initial filter to select  $^{114}\text{Ba}$  implants; subsequently, unambiguous identification can be achieved using the characteristic  $\alpha$ -decay energies and half-lives. Of particular importance in the identification of the  $^{114}\text{Ba}$   $\alpha$ -decay chain is the short half-life (relative to the neighboring nuclei and to the time between implantation events) of the granddaughter nucleus  $^{106}\text{Te}$ .

In the search for  $^{114}\text{Ba}$ , it was required that an implant ( $r_1$ ) occurred, followed by three successive decays ( $\alpha_1$ ,  $\alpha_2$ , and  $\alpha_3$ ) in the same pixel of the DSSD, and that all signals (implant plus three decays) were received within a 6-s period. It was initially required that  $\alpha_1$  was emitted within 1.6 s [ $\sim 4 \times T_{1/2}(^{114}\text{Ba})$ ] of  $r_1$ ,  $\alpha_2$  decay within 400 ms [ $\sim 4 \times T_{1/2}(^{110}\text{Xe})$ ] of  $\alpha_1$ , and  $\alpha_3$  within 0.3 ms [ $\sim 4 \times T_{1/2}(^{106}\text{Te})$ ] of  $\alpha_2$ . However, it was found that the selectivity was entirely based on the short (0.3-ms) time condition between  $\alpha_2$  and  $\alpha_3$ , so this condition alone was ultimately used. With this requirement between the times of  $\alpha_2$  and of  $\alpha_3$ , and with no conditions placed on the decay energies, a total of 17 events were selected. For these events, the energies of the first ( $\alpha_1$ ), second ( $\alpha_2$ ), and third ( $\alpha_3$ )  $\alpha$  decays recorded by the DSSD are shown in Figs. 2(a), 2(b), and 2(c), respectively. The spectrum for  $\alpha_1$ , which has been assigned to be the decay of  $^{114}\text{Ba}$ , exhibits a clear peak at energy 3480(20) keV. In the spectrum for  $\alpha_2$ , assigned to be the decay of  $^{110}\text{Xe}$ , several channels with two counts and a channel with four counts form an apparent peak with a centroid at 3720(20) keV. The spectrum for  $\alpha_3$ , assigned to the decay of  $^{106}\text{Te}$ , has counts that are more widely distributed, but with a number of counts between 3800 and 4200 keV: there are two counts in the channel corresponding to 3940 keV (10 keV per channel) with a cluster of counts at higher energy. The centroid of these counts is at 4100(60) keV.

The times between successive events in the chain  $r_1\alpha_1\alpha_2\alpha_3$  can be used to investigate the half-lives of each of the decays. Figures 3(a), 3(b), and 3(c) show the distributions of times between ( $r_1$  and  $\alpha_1$ ), ( $\alpha_1$  and  $\alpha_2$ ), and ( $\alpha_2$  and  $\alpha_3$ ), respectively. Application of the maximum-likelihood method [26,27] to

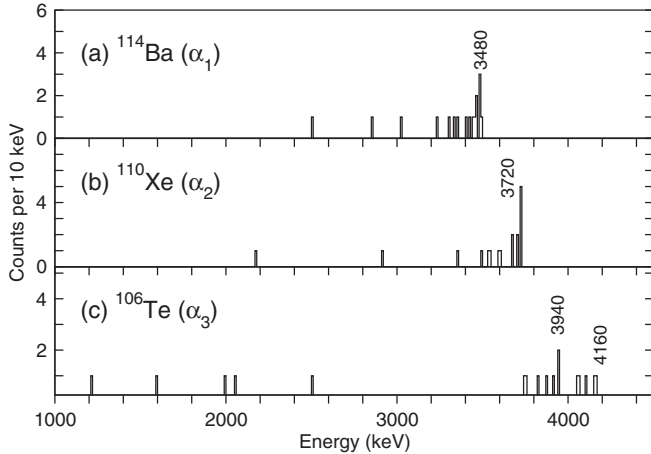


FIG. 2. Energy spectra from the DSSDs. Panels (a), (b), and (c) show the energies of the first ( $\alpha_1$ ), second ( $\alpha_2$ ), and third ( $\alpha_3$ ) decays when it is required that the decays occur following an implant, in the same pixel, and that  $\alpha_3$  occurs within 0.3 ms of  $\alpha_2$ . The values written vertically on the panels give the energies associated with selected channels, not the centroids.

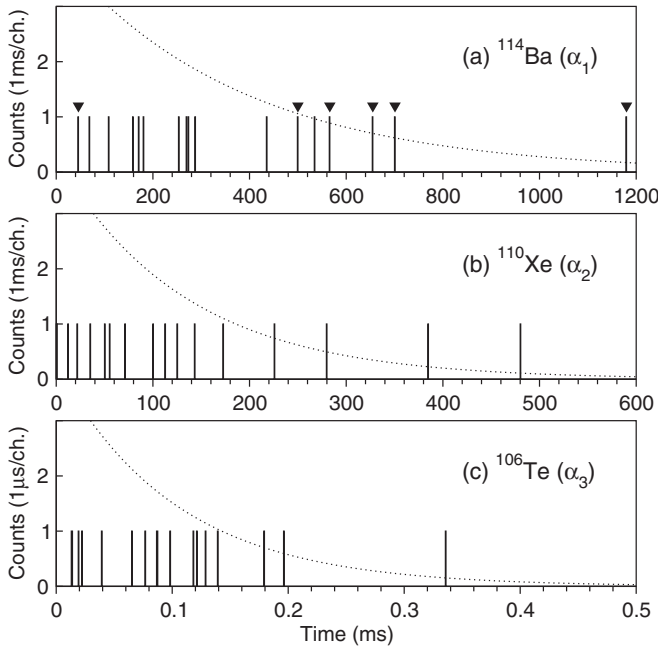


FIG. 3. The distributions of time differences between successive events in the DSSDs. Panel (a) shows the time differences between the implanted recoil ( $r_1$ ;  $^{114}\text{Ba}$ ) and the first decay ( $\alpha_1$ ). Panels (b) and (c) show the time differences between the first ( $\alpha_1$ ) and second ( $\alpha_2$ ) decays and between the second ( $\alpha_2$ ) and third ( $\alpha_3$ ) decays, respectively. The triangles on panel (a) label the data points which have been subjected to the condition that there must be a time difference of at least 1.6 s between the two implantation events immediately prior to the decay events, as described in the text. The dotted lines are calculated using the extracted half-lives, intended to show the decay behavior; they are not fits to the data.

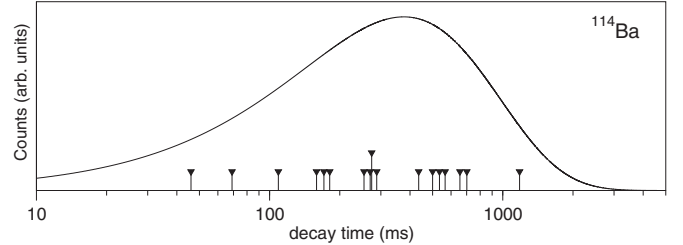


FIG. 4. The logarithmic decay-time distribution of all 17 events attributed to the  $^{114}\text{Ba} \rightarrow ^{110}\text{Xe}$   $\alpha$  decay. The curve shows the calculated logarithmic decay-time distribution as defined in Ref. [28] and the units on the vertical axis are arbitrary.

these data has allowed values for the half-lives to be extracted. For  $^{110}\text{Xe} (\alpha_2)$  the half-life is measured to be  $95^{+25}_{-20}$  ms and for  $^{106}\text{Te} (\alpha_3)$ , the half-life is  $70^{+20}_{-15}$   $\mu\text{s}$ . Measurement of the half-life of  $^{114}\text{Ba} (\alpha_1)$  is complicated by the possibility that  $\alpha_1$  is *not* emitted from  $r_1$ , but that it is emitted from a previous implant in the same pixel ( $r_0$ ), with  $r_1$  decaying by some mode other than  $\alpha$  decay. If this happens, the half-life extracted from the time between  $r_1$  and  $\alpha_1$  will give an incorrect value. In order to reduce this possibility, a condition has been applied such that the time between  $r_0$  and  $r_1$  must be greater than four times the (previously measured) half-life of  $^{114}\text{Ba}$ , or  $\sim 1.6$  s. In this case, if  $r_0$  is the  $^{114}\text{Ba}$  implant, then there is a 95% probability that it will decay before  $r_1$  occurs. This then significantly increases the probability that  $\alpha_1$  is indeed emitted from  $r_1$ . With this condition, there are 6 three- $\alpha$  events in the data, as marked by the triangles on Fig. 3(a). Subsequently, the half-life of  $^{114}\text{Ba} (\alpha_1)$  is extracted from these events to be  $380^{+190}_{-110}$  ms. It should be noted that the energy spectra of Fig. 2 do not use the condition on the time between  $r_0$  and  $r_1$ . However, this does not mean that the spectra are invalid; the three  $\alpha$  decays are still attributed to the most recent  $\alpha$ -decaying implant in the same pixel, but this is not necessarily the most recent implant. In order to test whether a set of data points from radioactive decay originate from a single radioactive species, a procedure has been defined by Schmidt which is described in Ref. [28]. In that work, the parameter  $\sigma_{\Theta \text{ exp}}$  is defined, and limits on this parameter are given within which there is a 90% confidence level that the events originate from the same single species. For the 17 events recorded here,  $\sigma_{\Theta \text{ exp}}$  is calculated to be 0.84, which lies within the limits of 0.78 and 1.74 for a data set of 17 events. This suggests that they do indeed arise from decay of the same radioactive species. Figure 4 shows the logarithmic decay-time distribution of all 17 events, plotted as suggested in Ref. [28]. For comparison, the half-life was also estimated from all 17 events, without the time condition between  $r_0$  and  $r_1$ , but with the correction defined by Leino *et al.* in Ref. [29]. The resulting half-life of  $\sim 400$  ms is very similar to that obtained here.

The number of  $^{114}\text{Ba}$   $\alpha$ -decay events, together with information about the beam intensity, target thickness, and detection efficiencies, has been used to estimate the production cross section for  $^{114}\text{Ba}$ . The transport efficiency of RITU was estimated by comparing the intensities of the same  $\gamma$  rays (from the  $2p$  and  $3p$  evaporation channels) in the  $\gamma\gamma\gamma$  and in

TABLE I. Properties of the  $\alpha$  decays of  $^{114}\text{Ba}$ ,  $^{110}\text{Xe}$ , and  $^{106}\text{Te}$  measured in the present work compared to previously measured values. The symbols  $T_{1/2}$ ,  $E_\alpha$ , and  $Q_\alpha$  represent the half-life,  $\alpha$ -particle energy, and  $\alpha$ -decay  $Q$  value, respectively. The data from this work are given as the first row for each nucleus. References are given for the previously measured values in subsequent rows.

Nucleus	$T_{1/2}$ (ms)	$E_\alpha$ (keV)	$Q_\alpha$ (keV)
$^{114}\text{Ba}$	$380^{+190}_{-110}$	3480(20)	3610(20)
	$430^{+300}_{-150}$ [17]	3410(40) [14]	3540(40) [14]
$^{110}\text{Xe}$	$95^{+25}_{-20}$	3720(20)	3860(20)
	$105^{+35}_{-25}$ [25]	3717(19) [4]	3856(20) [4]
$^{106}\text{Te}$	$0.070^{+0.020}_{-0.015}$	4100(60)	4260(60)
	$0.070^{+0.020}_{-0.010}$ [25]	4128(9) [31]	4290(9) [31]

the  $\gamma\gamma\gamma$ -recoil spectra. Here, it was necessary to use high-fold  $\gamma$ -ray spectra to meet the  $\gamma$ -ray fold requirement for data collection, and hence circumvent the bias that would be caused by the requirement of a DSSD signal. Using this method, the RITU transport efficiency was estimated to be around 30(5)%. In estimating the cross section, it was assumed that none of the  $\alpha$  particles emitted from the implanted nuclei escaped from the detector. Given the expected implantation depth and  $\alpha$ -particle ranges, this will be a reasonably good assumption. However, it is likely that a small percentage of the  $\alpha$  particles will escape, meaning that the estimate for the cross section is a lower limit. Taking all of this information into account, the cross section for  $^{114}\text{Ba}$  in this work was estimated to be 0.15(9)  $\mu\text{b}$ . The cross section reported in Refs. [16,17], with a higher beam energy of 284 MeV, is  $0.2^{+0.13}_{-0.09} \mu\text{b}$ , which is consistent with that reported here. Statistical-model calculations [30] predict that  $2n$  evaporation will be maximized for a beam energy of  $\sim 215$  MeV, with a cross section of 5  $\mu\text{b}$ . It should be stated, however, that such calculations are notoriously unreliable in reproducing absolute cross sections in this region.

## V. DISCUSSION

### A. Comparison to previous work

The  $\alpha$ -decay energies and half-lives measured in this work are presented in Table I, and are compared to previously measured values. The  $E_\alpha$  values measured here are 3480(20), 3720(20), and 4100(60) keV for the  $\alpha$  decays of  $^{114}\text{Ba}$ ,  $^{110}\text{Xe}$ , and  $^{106}\text{Te}$ , respectively. The  $E_\alpha$  value for  $^{114}\text{Ba}$  measured in this work has a smaller uncertainty and is 70 keV higher than that measured in Ref. [14]. The  $E_\alpha$  value for  $^{110}\text{Xe}$  from this work is very similar to that measured in Ref. [4]. For  $^{106}\text{Te}$ , the value measured here has a larger uncertainty than the previously measured value from Ref. [31]. This is due to the wider distribution of counts in the spectrum. However, within uncertainties, the value measured here is consistent with that from Ref. [31].

It can be seen from Fig. 2 that the distributions of counts in the DSSD energy spectra increase when going down the decay chain. This can perhaps be explained by a consideration

of the implantation depth and the ranges of the  $\alpha$  particles in the DSSD. Calculations with the code SRIM [32] suggest that the recoils are implanted at a depth of  $\sim 15 \mu\text{m}$  into the DSSD, and that the range of a 3.5 MeV  $\alpha$  particle is  $\sim 13 \mu\text{m}$ , whereas that for a 4-MeV  $\alpha$  particle is close to  $17 \mu\text{m}$ . It would therefore be expected that higher energy  $\alpha$  particles are more likely to escape from the silicon without depositing their full energy, which would contribute towards the wider distributions of counts in Fig. 2. Another effect that can contribute to the wide distribution of energies in the DSSD is the failure of the amplifier to return to the baseline following the preceding signal in the same DSSD strip; this effect has been shown to be significant for fast decays following an implantation event. In the present work, the possibility that the signal from the reasonably fast  $\alpha$  decay of  $^{106}\text{Te}$  ( $70 \mu\text{s}$ ) could be affected by the preceding  $\alpha$  decay ( $^{110}\text{Xe}$ ) was excluded by studying the correlations between  $\alpha$ -decay energies and decay times.

The half-lives are presented in Table I. For  $^{114}\text{Ba}$ , the value of half-life of  $380^{+190}_{-110} \text{ ms}$  measured in the present work is lower than the value of  $430^{+300}_{-150} \text{ ms}$  measured in Ref. [14], but is consistent within the large uncertainty of that value. For  $^{110}\text{Xe}$  the half-life measured here is  $95^{+25}_{-20} \text{ ms}$ ; this is consistent with the value of  $105^{+35}_{-25} \text{ ms}$  from Ref. [25]. For  $^{106}\text{Te}$ , the half-life measured here is  $70^{+20}_{-15} \mu\text{s}$ , which is similar to the value of  $70^{+20}_{-10} \mu\text{s}$  from Ref. [25].

It should be noted that in the present data, it was not possible to measure the  $\alpha$ -decay branching ratios ( $b_\alpha$ ) of  $^{114}\text{Ba}$  and  $^{110}\text{Xe}$ , since the observations of the  $\alpha$ -decay chains were necessary to select and identify these nuclei. Therefore, only the  $^{114}\text{Ba}$  and  $^{110}\text{Xe}$  nuclei that decayed by  $\alpha$ -particle emission were identified in the present work.

### B. Q values for $\alpha$ and $^{12}\text{C}$ emission

The  $Q$  values for  $\alpha$  decay ( $Q_\alpha$ ) deduced from this work are presented in Table I, in comparison to values from earlier work. A thorough discussion of the  $Q_\alpha$  value of  $^{114}\text{Ba}$  was presented in Ref. [14] in comparison to several different theoretical models. For example, the finite-range droplet model (FRDM) [33] predicts the  $Q_\alpha$  value of  $^{114}\text{Ba}$  to be 3550 keV, which is 60 keV lower than the value measured here but 10 keV higher than that of Ref. [14]. As pointed out in Ref. [14] the agreement between FRDM values and experimental values is progressively worse for  $^{110}\text{Xe}$  and  $^{106}\text{Te}$ , where the calculated values are 750 and 1750 keV too high, respectively.

The nucleus  $^{114}\text{Ba}$  has been identified as the most promising candidate in this region from which to observe  $^{12}\text{C}$  emission [8]. The calculated half-life for  $^{12}\text{C}$  emission depends sensitively on the  $Q$  value for this decay mode ( $Q_{^{12}\text{C}}$ ): an increase of 1 MeV in  $Q_{^{12}\text{C}}$  results in a half-life that is shorter by two orders of magnitude [34]. The value of  $Q_{^{12}\text{C}}$  can be deduced from the  $Q_\alpha$  values for the three successive  $\alpha$  decays that lead to the same final nucleus, with corrections for the binding energies of the three  $\alpha$  particles and of  $^{12}\text{C}$ . Using the data in Table I, a  $Q_{^{12}\text{C}}$  value of 19 035(45) keV is deduced for  $^{114}\text{Ba}$  in this work. This is slightly larger than the value of 19 000(40) keV from Refs. [14,18], as would be expected from the larger value of  $E_\alpha$ .

TABLE II. Reduced  $\alpha$ -decay widths ( $W_\alpha$ ) for  $^{114}\text{Ba}$ ,  $^{110}\text{Xe}$ , and  $^{106}\text{Te}$ , together with data used in their calculation. References to previous work are given in square brackets; where no reference is given, the data are taken from the present work.

Nucleus	$E_\alpha$ (keV)	$Q_\alpha$ (keV)	$b_\alpha$ (%)	$T_{1/2}$ (ms)	$W_\alpha$
$^{114}\text{Ba}$	3480(20)	3610(20)	0.9(3) [14]	$380^{+190}_{-110}$	$6^{+4}_{-3}$
$^{110}\text{Xe}$	3720(20)	3860(20)	64(35) [14]	$95^{+25}_{-20}$	$4^{+2}_{-2}$
$^{106}\text{Te}$	4128(9) [1]	4290(9) [1]	100 [14]	$0.070^{+0.020}_{-0.015}$	$4.4^{+1.2}_{-0.9}$

for  $^{114}\text{Ba}$  from the present work. The calculations presented in Ref. [34] suggest that this increase in the value of  $Q_{^{12}\text{C}}$  will reduce the half-life for  $^{12}\text{C}$  emission by about one month.

### C. Reduced widths

The reduced width for  $\alpha$  decay can be expressed by the quantity  $\delta^2$ , in units of MeV, as

$$\delta^2 = \lambda_\alpha h / P, \quad (1)$$

where  $h$  is Planck's constant,  $\lambda_\alpha$  is the partial decay constant for  $\alpha$  decay, and  $P$  is the  $\alpha$ -particle barrier penetrability, calculated using the method of Rasmussen [35]. The quantity  $\delta^2$  is often given relative to that for  $^{212}\text{Po}$ , as the dimensionless quantity  $W_\alpha$  which is defined as

$$W_\alpha = \frac{\delta^2}{\delta^2(^{212}\text{Po})}. \quad (2)$$

The values of  $W_\alpha$  calculated in the present work are given in Table II together with the data used in the calculations, assuming  $s$ -wave  $\alpha$ -particle emission. The value of  $E_\alpha$  for  $^{106}\text{Te}$  measured by Page *et al.* in Ref. [1] has a lower uncertainty than that measured here and has been adopted in the calculations. The values of  $W_\alpha$  for  $^{114}\text{Ba}$ ,  $^{110}\text{Xe}$ , and  $^{106}\text{Te}$  are all consistent within uncertainties. The value from the present work has an improved precision compared to the value of  $W_\alpha$  of  $16^{+12}_{-7}$  for  $^{114}\text{Ba}$  reported in Ref. [14], and in

general there is a better overlap of the three  $W_\alpha$  values in the decay chain. The relatively large uncertainties on these values mean, however, that it is difficult to draw any firm conclusions regarding the predictions of superallowed  $\alpha$  decay.

## VI. SUMMARY

In summary, the nucleus  $^{114}\text{Ba}$  has been produced in an experiment at the Accelerator Laboratory of the University of Jyväskylä Department of Physics, using the  $^{58}\text{Ni}(^{58}\text{Ni}, 2n)$  reaction, with a beam energy of 210 MeV. Following implantation into DSSDs at the focal plane of the RITU recoil separator, position and time correlations have been used to identify 17 events in the  $^{114}\text{Ba} \rightarrow ^{110}\text{Xe} \rightarrow ^{106}\text{Te} \rightarrow ^{102}\text{Sn}$  triple  $\alpha$ -decay chain. The energy of the  $^{114}\text{Ba} \alpha$  decay has been measured to be 3480(20) keV, which is 70 keV higher than the previously measured value [14]. The half-life of  $^{114}\text{Ba}$  has been measured to be  $380^{+190}_{-110}$  ms; this is consistent with the previous measurement, but with improved accuracy. A revised value for  $Q_{^{12}\text{C}}$  of 19035(45) keV is put forward. The cross section for the reaction has been estimated to be  $0.15(9) \mu\text{b}$ . This cross section suggests that it may be possible to successfully identify the low-lying excited states of  $^{114}\text{Ba}$  in a future dedicated experiment. Such an experiment would benefit from  $A/q$  separation of the reaction products as will be available using, for example, the MARA vacuum-filled recoil separator [36], which is presently under development at the University of Jyväskylä.

## ACKNOWLEDGMENTS

This work has been supported by the Science and Technology Facilities Council (UK), the EU 7th Framework Programme “Integrating Activities—Transnational Access” Project No. 262010 (ENSAR) and by the Academy of Finland under the Finnish Centre of Excellence Programme (Nuclear and Accelerator Based Physics Programme at JYFL; Contract No. 213503). The authors acknowledge support of Gammapool for the loan of the Jurogam HPGe detectors.

- 
- [1] R. D. Page, P. J. Woods, R. A. Cunningham, T. Davinson, N. J. Davis, A. N. James, K. Livingston, P. J. Sellin, and A. C. Shotter, *Phys. Rev. C* **49**, 3312 (1994).
  - [2] E. S. Paul, P. J. Woods, T. Davinson, R. D. Page, P. J. Sellin, C. W. Beausang, R. M. Clark, R. A. Cunningham, S. A. Forbes, D. B. Fossan, A. Gizon, J. Gizon, K. Hauschild, I. M. Hibbert, A. N. James, D. R. LaFosse, I. Lazarus, H. Schnare, J. Simpson, R. Wadsworth, and M. P. Waring, *Phys. Rev. C* **51**, 78 (1995).
  - [3] B. Hadinia, B. Cederwall, J. Blomqvist, E. Ganioglu, P. T. Greenlees, K. Andgren, I. G. Darby, S. Eeckhaudt, E. Ideguchi, P. M. Jones, D. T. Joss, R. Julin, S. Juutinen, S. Ketelhut, K. Lagergren, A.-P. Leppänen, M. Leino, M. Nyman, J. Pakarinen, E. S. Paul, M. Petri, P. Rahkila, M. Sandzelius, J. Sarén, C. Scholey, J. Uusitalo, R. Wadsworth, and R. Wyss, *Phys. Rev. C* **72**, 041303 (2005).
  - [4] M. Sandzelius, B. Hadinia, B. Cederwall, K. Andgren, E. Ganioglu, I. G. Darby, M. R. Dimmock, S. Eeckhaudt, T. Grahn,
  - P. T. Greenlees, E. Ideguchi, P. M. Jones, D. T. Joss, R. Julin, S. Juutinen, A. Khaplanov, M. Leino, L. Nelson, M. Niikura, M. Nyman, R. D. Page, J. Pakarinen, E. S. Paul, M. Petri, P. Rahkila, J. Saren, C. Scholey, J. Sorri, J. Uusitalo, R. Wadsworth, and R. Wyss, *Phys. Rev. Lett.* **99**, 022501 (2007).
  - [5] P. T. Wady, J. F. Smith, E. S. Paul, B. Hadinia, C. J. Chiara, M. P. Carpenter, C. N. Davids, A. N. Deacon, S. J. Freeman, A. N. Grint, R. V. F. Janssens, B. P. Kay, T. Lauritsen, C. J. Lister, B. M. McGuirk, M. Petri, A. P. Robinson, D. Seweryniak, D. Stepenbeck, and S. Zhu, *Phys. Rev. C* **85**, 034329 (2012).
  - [6] R. D. Macfarlane and A. Siivola, *Phys. Rev. Lett.* **14**, 114 (1965).
  - [7] D. N. Poenaru, D. Schnabel, W. Greiner, D. Mazilu, and R. Gherghescu, *At. Data Nucl. Data Tables* **48**, 231 (1991).
  - [8] D. N. Poenaru, W. Greiner, and E. Hourani, *Phys. Rev. C* **51**, 594 (1995).

- [9] A. Guglielmetti, B. Blank, R. Bonetti, Z. Janas, H. Keller, R. Kirchner, O. Klepper, A. Piechaczek, A. Plochocki, G. Poli, P. B. Price, E. Roeckl, K. Schmidt, J. Szerypo, and A. J. Westphal, *Nucl. Phys. A* **583**, 867 (1995).
- [10] A. Guglielmetti, R. Bonetti, G. Poli, P. B. Price, A. J. Westphal, Z. Janas, H. Keller, R. Kirchner, O. Klepper, A. Piechaczek, E. Roeckl, K. Schmidt, A. Plochocki, J. Szerypo, and B. Blank, *Phys. Rev. C* **52**, 740 (1995).
- [11] I. H. Lazarus, D. E. Appelbe, P. A. Butler, P. J. Coleman-Smith, J. R. Cresswell, S. J. Freeman, R. D. Herzberg, I. Hibbert, D. T. Joss, S. C. Letts, V. F. E. Pucknell, P. H. Regan, J. Sampson, J. Simpson, J. Thornhill, and R. Wadsworth, *IEEE Trans. Nucl. Sci.* **48**, 567 (2001).
- [12] S. N. Liddick, R. Grzywacz, C. Mazzocchi, R. D. Page, K. P. Rykaczewski, J. C. Batchelder, C. R. Bingham, I. G. Darby, G. Drafta, C. Goodin, C. J. Gross, J. H. Hamilton, A. A. Hecht, J. K. Hwang, S. Illyushkin, D. T. Joss, A. Korgul, W. Królas, K. Lagergren, K. Li, M. N. Tantawy, J. Thomson, and J. A. Winger, *Phys. Rev. Lett.* **97**, 082501 (2006).
- [13] I. G. Darby, R. K. Grzywacz, J. C. Batchelder, C. R. Bingham, L. Cartegni, C. J. Gross, M. Hjorth-Jensen, D. T. Joss, S. N. Liddick, W. Nazarewicz, S. Padgett, R. D. Page, T. Papenbrock, M. M. Rajabali, J. Rotureau, and K. P. Rykaczewski, *Phys. Rev. Lett.* **105**, 162502 (2010).
- [14] C. Mazzocchi, Z. Janas, L. Batist, V. Belleguic, J. Doring, M. Gierlik, M. Kapica, R. Kirchner, G. A. Lalazissis, H. Mahmud, E. Roeckl, P. Ring, K. Schmidt, P. J. Woods, and J. Zylicz, *Phys. Rev. B* **532**, 29 (2002).
- [15] Yu. Ts. Oganessian, Yu. A. Lazarev, V. L. Mikheev, Yu. A. Muzychka, I. V. Shirokovsky, S. P. Tretyakova, and V. K. Utyonkov, *Z. Phys. A* **349**, 341 (1994).
- [16] A. Guglielmetti, R. Bonetti, G. Poli, R. Collatz, Z. Hu, R. Kirchner, E. Roeckl, N. Gunn, P. B. Price, B. A. Weaver, A. Westphal, and J. Szerypo, *Phys. Rev. C* **56**, R2912(R) (1997).
- [17] Z. Janas, A. Płochocki, J. Szerypo, R. Collatz, Z. Hu, H. Keller, R. Kirchner, O. Klepper, E. Roeckl, K. Schmidt, R. Bonetti, A. Guglielmetti, G. Poli, and A. Piechaczek, *Nucl. Phys. A* **627**, 119 (1997).
- [18] C. Mazzocchi, Z. Janas, L. Batist, V. Belleguic, J. Doring, M. Gierlik, M. Kapica, R. Kirchner, G. A. Lalazissis, H. Mahmud, E. Roeckl, P. Ring, K. Schmidt, P. J. Woods, and J. Zylicz, *Acta Phys. Hung. N. S.* **18**, 345 (2003).
- [19] L. Capponi, J. F. Smith, P. Ruotsalainen, C. Scholey, P. Rahkila, B. Hadinia, K. Auranen, L. Bianco, A. J. Boston, H. C. Boston, D. M. Cullen, X. Derkx, M. Drummond, T. Grahn, P. T. Greenlees, L. Grocott, U. Jakobsson, D. T. Joss, R. Julin, S. Juutinen, M. Labiche, M. Leino, K. Leach, C. McPeake, K. F. Mulholland, P. Nieminen, D. O'Donnell, E. S. Paul, P. Peura, M. Sandzelius, J. Saren, B. Saygi, J. Sorri, S. Stolze, A. Thorntwaite, M. J. Taylor, and J. Uusitalo (unpublished).
- [20] L. Capponi, Ph.D. thesis, University of the West of Scotland, Paisley, UK, 2014.
- [21] P. J. Nolan, *Nucl. Phys. A* **520**, 657c (1990).
- [22] M. Leino, J. Åystö, T. Enqvist, P. Heikkinen, A. Jokinen, M. Nurmia, A. Ostrowski, W. H. Trzaska, J. Uusitalo, K. Eskola, P. Armbruster, and V. Ninov, *Nucl. Instrum. Methods Phys. Res., Sect. B* **99**, 653 (1995).
- [23] R. D. Page, A. N. Andreyev, D. E. Appelbe, P. A. Butler, S. J. Freeman, P. T. Greenlees, R.-D. Herzberg, D. G. Jenkins, G. D. Jones, P. Jones, D. T. Joss, R. Julin, H. Kettunen, M. Leino, P. Rahkila, P. H. Regan, J. Simpson, J. Uusitalo, S. M. Vincent, and R. Wadsworth, *Nucl. Instrum. Methods Phys. Res., Sect. B* **204**, 138 (2003).
- [24] P. Rahkila, *Nucl. Instrum. Methods Phys. Res., Sect. A* **595**, 637 (2008).
- [25] Z. Janas, C. Mazzocchi, L. Batist, A. Blazhev, M. Górska, M. Kavatsyuk, O. Kavatsyuk, R. Kirchner, A. Korgul, M. La Commara, K. Miernik, A. Płochoki, E. Roeckl, and K. Schmidt, *Eur. Phys. J. A* **23**, 197 (2005).
- [26] K.-H. Schmidt, C.-C. Sahm, K. Pielenz, and H.-G. Clerc, *Z. Phys. A* **316**, 19 (1984).
- [27] W. J. McBride, *IEEE Trans. Nucl. Sci.* **15**, 350 (1968).
- [28] K.-H. Schmidt, *Eur. Phys. J. A* **8**, 141 (2000).
- [29] M. E. Leino, S. Yashita, and A. Ghiorso, *Phys. Rev. C* **24**, 2370 (1981).
- [30] A. Gavron, *Phys. Rev. C* **21**, 230 (1980).
- [31] R. D. Page, P. J. Woods, R. A. Cunningham, T. Davinson, N. J. Davis, A. N. James, K. Livingston, P. J. Sellin, and A. C. Shotter, *Phys. Rev. Lett.* **72**, 1798 (1994).
- [32] SRIM (Stopping and Range of Ions in Matter) [<http://www.srim.org>].
- [33] P. Möller, J. R. Nix, and K.-L. Kratz, *At. Data Nucl. Data Tables* **66**, 131 (1997).
- [34] D. N. Poenaru, W. Greiner, and E. Hourany, *J. Phys. G: Nucl. Part. Phys.* **22**, 621 (1996).
- [35] J. O. Rasmussen, *Phys. Rev.* **113**, 1593 (1959).
- [36] J. Sarén, J. Uusitalo, M. Leino, P. T. Greenlees, U. Jakobsson, P. Jones, R. Julin, S. Juutinen, S. Ketelhut, M. Nyman, P. Peura, P. Rahkila, C. Scholey, and J. Sorri, *Nucl. Instrum. Methods Phys. Res., Sect. B* **266**, 4196 (2008).